Journal of Applied Polymer Science

Orthogonal design study on factors affecting the diameter of perfluorinated sulfonic acid nanofibers during electrospinning

Tiandan Song,[1] Zhiyuan Chen,[1] Hong He,[1] Yuexing Liu,[1] Yong Liu,[1] Seeram Ramakrishna[2]
[1]College of Mechanical and Electric Engineering, Beijing University of Chemical Technology, Beijing 100029, China
[2]Nanoscience and Nanotechnology Initiative, National University of Singapore, Singapore 117576, Singapore
Correspondence to: Y. Liu (E-mail: yongsd@iccas.ac.cn)

ABSTRACT: In this study, Nafion® NR 40 beads with polyethylene oxide (PEO) are fabricated into a nanofiber membrane using electrospinning. In particular, Nafion® beads in non-toxic mixed solvent (EtOH and H_2O) were blended with the carrier polymer PEO, which is the minor component in the solution responsible for the solution spinnability. The highest content of Nafion® in the nanofiber is 98.04%. To investigate the factors influencing the nanofiber diameter during electrospinning, an orthogonal design method was adopted. These factors include the carrier polymer content, distance between the syringe needle and roller collector, flow rate of the electrospinning solution, and the roller rotation speed. After obtaining the significant factors and optimal test level, an additional optimization experiment is conducted under the best conditions. The resulting nanofibers have a diameter of ~150 nm. Moreover, the obtained Nafion® nanofiber membrane has strong potential for applications in polymer electrolyte membrane fuel cells (PEMFC), the chlor-alkali industry, catalysts, and metal ion removal. © 2014 Wiley Periodicals, Inc. J. Appl. Polym. Sci. **2015**, *132*, 41755.

KEYWORDS: batteries and fuel cells; electrospinning; membranes

Received 30 August 2014; accepted 31 October 2014
DOI: 10.1002/app.41755

INTRODUCTION

Perfluorinated sulfonic acid (PFSA) polymer, which is a solid super acid containing a large number of sulfonic acid groups, has been extensively used in polymer electrolyte membrane fuel cells (PEMFC),[1–3] chlor-alkali industry,[4] catalysts,[5] metal ion removal,[6] and other areas. However, PFSA is most commonly used in melt extrusion films or solution casting films.[7] In particular, Nafion® membranes from DuPont have shown high proton conductivity under fully hydrated conditions.[8] Unfortunately, the fabrication of melt extrusion films is patented by several companies, leading to the high cost of these films. In addition, the production of solution casting films requires a considerable length of time to evaporate the solvent. Moreover, pinholes frequently develop in the membranes produced by melt extrusion or solution casting, and these serious defects can result in widespread damage and reduce the production of quality membranes.[9] To prevent above defects from developing, several researchers have proposed a new method for producing PFSA membranes using electrospinning nanofibers.

Electrospinning is an easy and useful method for fabricating nanofibers.[10,11] Because of the fast development of electrospinning processes and the many potential applications of the electrospun nanofibers, the quality especially the diameter of electrospun fibers has drawn increasing attention.[12,13] Ballengiee *et al.* fabricated Nafion® and polyphenylsulfone (PPSU) membranes by simultaneously electrospinning Nafion® (solution) and PPSU into a dual-fiber mat and then examined the various processing steps for transforming the dual-fiber electrospun mat into a functional proton exchange membranes (PEM).[14–16] Laforgue found that the PFSA nanofiber membrane has good proton conductivity, water retention, dimensional changes, and other excellent properties when compared with commercial Nafion® film.[17] However, numerous problems had to be addressed to obtain enhanced functional nanofibers, including enhancing the purity of PFSA nanofibers and decreasing their diameter. Previously, Dong successfully obtained high-purity (99.9 wt %) PFSA nanofibers.[18] The average fiber diameter increased from 125 to 400 nm when the content of Nafion® was increased from 98 to 99.9 wt %. The material used in the study described above is a type of commercial Nafion® solution. In the present study, to obtain very fine, high-purity nanofibers, we used bead-form Nafion® to form the electrospinning solution. Bead-form Nafion® has become a common form of this polymer material owning to many advantages, such as convenient transportation and storage. Moreover, porous Nafion® nanofibers have been successfully obtained using electrospinning method.[19,20] Previous studies have shown that thermal treating led to the formation of uniform pore structure and pore size distribution, lower pore size as well as smaller surface

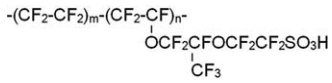

Scheme 1. The chemical structure of Nafion®.

roughness.[21–23] After thermal compression or solution evaporation, the nanofiber layer should form a uniform membrane, eliminating pinholes if the nanofibers are evenly distributed.

High-performance PFSA membranes can only be achieved by fabricating high-quality PFSA nanofibers. Thus, studying preparation methods for PFSA nanofibers is an important endeavor. However, numerous factors such as solution concentration, length of polymer chains, voltage, distance, and inner-diameter of spinning needle affect the electrospinning process. To comprehensively study these factors, we adopt an orthogonal design method to compare the effectiveness of multiple intervention components and to examine the influence of spinning factors on the nanofiber diameter during electrospinning.[24,25] These factors mainly include the content of carrier polymer, distance between the syringe needle and the roller collector, flow rate of electrospinning solution, and the rotation speed of the roller. This method can reduce test times as well as clarify the relationship between the factors and the experimental indexes.[26–28] The significant factors and optimal test level can then be determined using the analysis of the results. Based on the significant factor and the optimal test level, further optimization have been performed to verify the method and to enhance nanofiber quality.

EXPERIMENTAL

Materials

Nafion® NR 40 (bead-form, IEC = 1.0 meq g^{-1}, M_w = 544.1391 g mol^{-1}) purchased from DuPont, was a copolymer of tetrafluoroethylene and perfluoro-3, 6-dioxa-4-methyl-7-octenesulfonyl fluoride, converted to the proton (H+) form. The chemical structure of Nafion® was shown in Scheme 1. Polyethylene oxide (PEO; M_w = 5.10v6 g mol^{-1}), purchased from the Dow Chemical, ethanol (EtOH; AR), purchased from Beijing Modern Oriental Fine Chemistry, and Nafion® beads were used as received without any further purification. H_2O was distilled in laboratory. Just as Table I shows.

Equipment

Figure 1 shown the electrospinning apparatus used in this study. The syringe pump was used to feed the spinning solution and to control the flow rate accurately. The lifter under the syringe pump could adjust the height of the pump according to the requirements of the experiment. The roller collector was applied to collect continuous nanofibers to achieve a uniform film. The

Table I. The Detailed Specifications of all Applied Chemicals

Main materials	Nafion® NR 40, bead-form, M_w = 544.1391 g mol^{-1}
Carrier polymer	Polyethylene oxide (PEO), M_w = 5.10v6 g mol^{-1}
Solvent	Ethanol (EtOH), AR; H_2O, distilled water

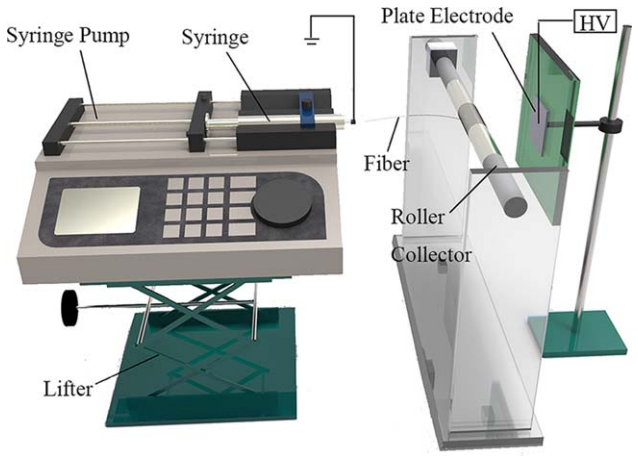

Figure 1. Apparatus used for electrospinning. [Color figure can be viewed in the online issue, which is available at wileyonlinelibrary.com.]

roller collector employed insulated resin as roller and acrylic glass as holder. The roller was driven by the infinitely variable speed DC motor, such that the rotation speed could be adjusted as needed. On the right side of the roller collector was the plate electrode, which was connected to the anode of the high-voltage generator. Meanwhile, the needle of the syringe was grounded as cathode.

Experimental Design

To obtain thin nanofibers with high purity, we focused on the factors of the whole electrospinning process. Given that pure PFSA had short chain; its solution had insufficient chain entanglement to be spun into fibers.[6] Thus, carrier polymer (PEO) should be added to enhance chain entanglement. In this research, non-toxic mixed solvent (EtOH and H_2O) were used. EtOH quickly evaporated from the surface of nanofibers during the spinning process because of its high volatility, whereas H_2O enhanced the polarity of the solution to dissolve the strong polar PFSA particles.

Numerous factors influenced the quality of nanofibers during electrospinning. Such factors included solution system, solution viscosity, electrospinning voltage, temperature, flow rate, inner diameter of needle, the distance between syringe needle and collector, receiver shape, etc. In the solution system, we only changed the carrier polymer content (PEO). In addition, the PFSA content in nanofibers exceeded 95 wt % after adding the PEO. The orthogonal table L_9 ([34]) was adopted to arrange the experiments. The number "4" stood for four factors, "3" for three levels, and "9" for nine trials. Factors shown in Tables II and III included the contents of carrier polymer (PEO), distance between the syringe needle and the roller collector, flow rate, and rotation speed of the roller collector.

Solution Preparation

First, 2 g of PFSA, 32 g of EtOH and 8 g of H_2O were added into an airtight high pressure reactor and stirred at 160°C for 4 h. Second, we added carrier polymer PEO in different levels (0.04, 0.07, and 0.1 g) into the above solution after the solution temperature was reduced to 25°C and then stirred for 8 h at room temperature. The mass (g) ratio of the solution system

Table II. Contents of Orthogonal Factors and Their Levels

Factor level	Content of carrier polymer (A) (g)	Distance between syringe needle and roller collector (B) (cm)	Flow rate (C) (mL h^{-1})	Rotate speed of roller collector (D) (r min^{-1})
1	0.1	17	0.1	60
2	0.07	20	0.3	120
3	0.04	23	0.5	180

Four factors and three levels of each factor.

Table III. Effect of Four Factors on Fiber Diameter

	Parameters		Measured property		
Trial no.	Content of carrier polymer (A) (g)	Distance between syringe needle and roller collector (B) (cm)	Flow rate (C) (mL h^{-1})	Rotate speed of roller collector (D) (r min^{-1})	Diameter of fibers (nm)
1	0.1	17	0.1	60	1757
2	0.1	20	0.3	120	5622
3	0.1	23	0.5	180	4937
4	0.07	17	0.3	180	2423
5	0.07	20	0.5	60	7521
6	0.07	23	0.1	120	1317
7	0.04	17	0.5	120	5239
8	0.04	20	0.1	180	2124
9	0.04	23	0.3	60	2600
k1	4105.333	3139.667	1732.667	3959.333	
k2	3753.667	5089.000	3548.333	4059.333	
k3	3321.000	2951.333	5899.000	3161.333	
R	784.333	2137.667	4166.333	898.000	

The conditions of these nine trials were carried out according to the requirements of orthogonal table. The diameter of fibers was measured by Image J. The *k*1, *k*2, *k*3, and *R* were results of the range analysis.

was ethanol : water : Nafion® : PEO = 32 : 8: 2: (0.04, 0.07, and 0.1). Finally, the mixture was left to stand at room temperature for 4 h to ensure become homogeneity.

Electrospinning

Spinning voltage was determined after trial and error, combined with the requirement for distance and flow rate, which were required to enable the nanofibers to reach the roller collector and for these nanofibers to be homogeneously continuous. The spinning voltage was 20 KV, the inner diameter of needle was 0.5 mm, and the distance between the roller collector and the plate electrode was 6 cm.

Table IV. Experimental Arrangements in Calculating k^A value

Group	A	B	C	D
1 (Trial No. 1, 2, 3)	All A_1	B_1 once; B_2 once; B_3 once	C_1 once; C_2 once; C_3 once	D_1 once; D_2 once; D_3 once
2 (Trial No. 4, 5, 6)	All A_2	B_1 once; B_2 once; B_3 once	C_1 once; C_2 once; C_3 once	D_1 once; D_2 once; D_3 once
3 (Trial No. 7, 8, 9)	All A_3	B_1 once; B_2 once; B_3 once	C_1 once; C_2 once; C_3 once	D_1 once; D_2 once; D_3 once

Nos. 1–9 were same to Table III, A stands for the content of carrier polymer, B stands for distance between syringe needle and roller collector, C stands for flow rate, D stands for the rotation speed of the roller.

Measurements and Analyses

SEM images of nanofibers were obtained by using HITACHI SU1510 and HITACHI S4700 equipment. The mean diameter was calculated by using Image J (National Institutes of Health). In each image, 30 nanofibers were measured, and three points were extracted in every nanofiber to obtain 90 data points from each image. The data were then averaged. Finally, range analysis was applied to the experimental results by using the orthogonal design method.

RESULTS AND DISCUSSION

Through the orthogonal design method, the content of carrier polymer, distance between syringe needle and roller collector,

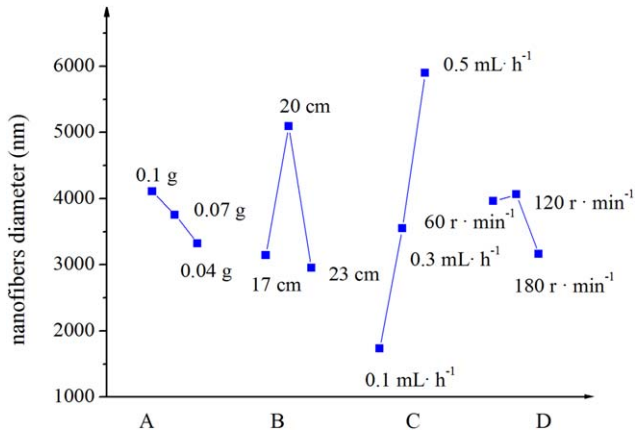

Figure 2. Influence of four factors on average fiber diameter. [Color figure can be viewed in the online issue, which is available at wileyonlinelibrary.com.]

flow rate and the rotation speed of the roller were tested. We take factor A as an example for analysis, as shown in Table IV.

First, the experiments (trial Nos. 1, 2, and 3) containing factor A level "1" (A1) were placed in group 1. Similarly, factor A levels "2" and "3" (A2, A3) were placed in groups 2 and 3, respectively. In this way, A1, A2, and A3 appeared thrice in each group, whereas levels 1, 2, and 3 of other factors B, C, and D, respectively, appeared only once. The experimental results of the three groups were summarized and their average was computed; for example, $k_1^A = (x1 + x2 + x3)/3 = (1757 + 5622 + 4937)/3 = 4105.333$. k_2^A and k_3^A were calculated in the same way. When we compared k_1^A, k_2^A, k_3^A, we considered that the influence of other factors B, C, and D were approximately the same. From the three groups, we consider that the value of k^A reflects thrice the effect of factor A and once that of factors B, C, and D. Thus, the differences among k_1^A, k_2^A, and k_3^A only resulted from the three different levels of factor A. The difference between the maximum and minimum of k_1^A, k_2^A and k_3^A was range R_A. The k and R of B, C, and D can be derived as well, as shown in Table III. The factor would exert a stronger influence on the index, that is, the diameter value, when R is larger. The maximum of R corresponds to the dominant factor. In this study, we aimed for the nanofiber diameter to be as small as possible. Hence, the minimum value among k_1, k_2, and k_3 corresponds to the required level. Figure 2 shows four curves, with the lowest level of each curve being the optimal level.

A comparison of the R values of Table III gives the result $R_C > R_B > R_D > R_A$. This result shows that the influence of the four factors on the average nanofiber diameter can be listed in the following order: flow rate > distance between the syringe needle and the roller collector > rotation speed of the roller > content of carrier polymer. Figure 2 reveals that the optimal points were A_3, B_3, C_1, and D_3, which correspond to a carrier polymer content of 0.04 g, distance between the syringe needle and roller collector of 23 cm, flow rate of 0.1 mL h^{-1}, and rotation speed of the roller of 180 r min^{-1}.

Flow rate is the main factor influencing nanofiber diameter. Figure 3 shows that the nanofiber diameter is significantly smaller than the other two diameters in the same line when the flow rate is 0.1 mL h^{-1}, (Nos. 1, 6, and 8 in the image) possibly because when the flow rate is low, the molecular chain in the solution can be better stretched and oriented in the electric field. In addition, the low flow rate contributes to strong jet whipping because the electric field force easily drives the light jet movement. Whipping is important to obtain thin

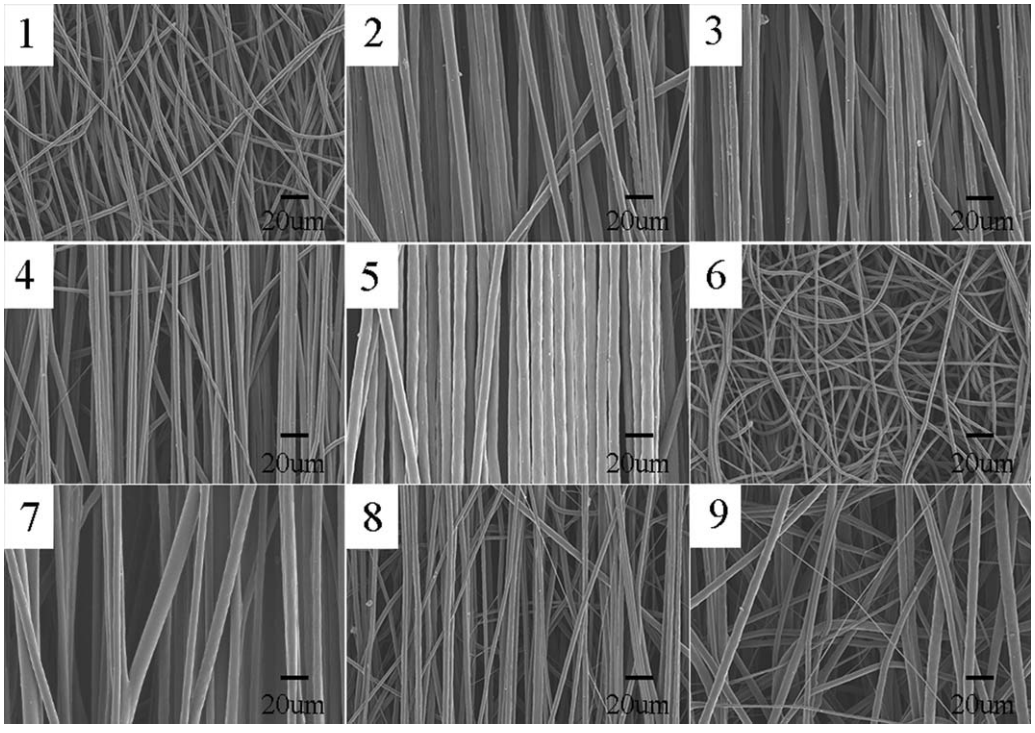

Figure 3. SEM images of nanofibers corresponding to the nine trials.

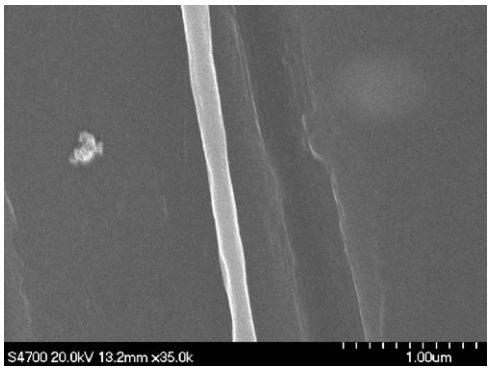

Figure 4. The nanofibers SEM image of optimization experiment.

fibers. Figure 3 shows the disordered nanofibers obtained on the roller collector. Meanwhile, a large flow rate weakens jet whipping. Combined with the tensile force of the roller, the nanofiber tends to be stretched and highly oriented, as shown in No. 5 of Figure 3, in which the flow rate is 0.5 mL h^{-1}. In this study, we expected to obtain disordered nanofibers to ensure desirable mechanical properties of the membrane. The membrane easily cracked because it is made up of highly oriented nanofibers.

The second factor that affects nanofiber diameter is the distance between the syringe needle and the roller collector. This factor directly affects the electric force and the flying time of the nanofiber. Under the same voltage, a short distance between the syringe needle and the roller collector would engender stronger electric field intensity, thus resulting in smaller nanofiber diameter. Meanwhile, a long distance between the syringe needle and the roller collector increases the flying time of the nanofiber. From curve B in Figure 2, a peak is observed when the distance is 20 cm. This level is the worst among all levels and thus results in the largest fiber diameter. This finding indicates that the electric field intensity and flying time of nanofiber are not optimal. Given that the electric field intensity and flying time are inversely related to distance, several experiments are needed to identify the correct distance.

The rotation speed of the roller has a weak influence on nanofiber diameter. In a previous study, taking the roller as collector aimed at obtaining highly oriented nanofibers. Meanwhile, the present study aims to obtain continuous nanofibers and distribute them uniformly in a plane by using the roller collector, such that the nanofibers can fabricate homogeneous membrane by cutting the fiber cylinder into a rectangle. From the curve D in Figure 2, we can conclude that at the maximum speed of 180 r min^{-1}, the nanofiber diameter is the minimum. If the roller speed is slower than 180 r min^{-1}, the nanofiber diameter will be higher than the minimum, which will decrease the mechanical strength of a membrane in a certain direction. No obvious difference in nanofiber diameter is observed when the rotation speed is 60 or 120 r min^{-1}.

The third factor affecting nanofiber diameter is the carrier polymer content. Carrier polymer can promote the chain entanglement and make the blended solution spinnable. However, this condition will reduce the conductivity of PFSA nanofiber membrane and will complicate the membrane-forming process because the carrier polymer will be removed during post processing. Thus, to obtain high-purity PFSA nanofibers, we must reduce the carrier polymer content to the least possible amount. In this study, the PEO content is quite low, such that no obvious differences in fiber diameter were observed when the content changed. From curve A in Figure 2, the diameter was the smallest when the PEO content was the minimum. Thus, for this factor, 0.04 g is the optimal level.

From the analysis of our experiment results, we conducted the further optimization experiment by applying the optimal experimental conditions to verify whether finer fibers can be obtained. The electrospinning conditions are listed as follows: carrier polymer content, 0.04 g; distance between the syringe needle and the roller collector, 23 cm; flow rate, 0.1 mL h^{-1}; and rotation speed of the roller, 180 r min^{-1}. The other conditions were kept the same. Finally, we achieved improved nanofibers with an average diameter of ~150 nm. The SEM images of the nanofibers are shown in Figure 4.

CONCLUSION

We investigated the electrospinning factors of a PFSA/PEO/EtOH/H_2O system using the orthogonal design method, and we found that the four considered factors influenced the average nanofiber diameter in the following order: flow rate > distance between the syringe needle and roller collector > roller rotation speed > carrier polymer content. The optimal conditions were 0.04 g carrier polymer content, 23 cm distance between the syringe needle and roller collector, 0.1 mL h^{-1} flow rate, and 180 r min^{-1} roller rotation speed. These conditions were further used to optimize the fiber diamter. The resulting nanofibers had a diameter of ~150 nm, indicating that our proposed orthogonal design method is suitable and advantageous.

ACKNOWLEDGMENTS

The authors thank Professor Xiaozhen Yang of Institute of Chemistry, Chinese Academy of Science (ICCAS) for his valuable discussions. The article was financially supported by the National Natural Science Foundations of China (Grant Number 21374008).

REFERENCES

1. Mauritz, K. A.; Moore, R. B. *Chem. Rev.* **2004**, *104*, 4535.
2. Zhu, Y.; Mai, J.; Li, H.; Tang, J. K.; Yuan, W. Z.; Zhang, Y. M. *Polym. Degrad. Stabil.* **2014**, *107*, 106.
3. Peighambardoust, S. J.; Rowshanzamir, S.; Amjadi, M. *Int. J. Hydrogen Energy* **2010**, *35*, 9349.
4. Mohammadi, F.; Rabiee, A. *J. Appl. Polym. Sci.* **2011**, *120*, 3469.
5. Chang, X. F.; Hu, Y.; Xu, Z. L. *Mater. Lett.* **2011**, *65*, 1719.
6. Zhao, J. H.; Yuan, W. Z.; Xu, A. H.; Ai, F.; Lu, Y. W.; Zhang, Y. M. *React. Funct. Polym.* **2011**, *71*, 1102.
7. Cui, Z. L.; Drioli, E.; Lee, Y. M. *Prog. Polym. Sci.* **2014**, *39*, 164.
8. Wycisk, R.; Pintauro, P. N.; Park, J. W. *Curr. Opin. Chem. Eng.* **2014**, *4*, 71.

9. Moukheiber, E.; Bas, C.; Flandin, L. *Int. J. Hydrogen Energy* **2014**, *39*, 2717.
10. Camposeo, A.; Greenfeld, I.; Tantussi, F.; Pagliara, S.; Moffa, M.; Fuso, F. *Nano Lett.* **2013**, *13*, 5056.
11. Nayak, R.; Padhye, R.; Kyratzis, I. L.; Truong, Y. B.; Arnold, L. *Text. Res. J.* **2011**, *82*, 129.
12. Yu, D. G.; Yu, J. H.; Chen, L.; Williams, G. R.; Wang, X. *Carbohydr. Polym.* **2012**, *90*, 1016.
13. Yu, D. G.; Branford-White, C.; Annie Bligh, S. W.; White, K.; Chatterton, N. P.; Zhu, L. M. *Macromol. Rapid. Commun.* **2011**, *32*, 744.
14. Ballengee, J. B.; Pintauro, P. N. *J. Membr. Sci.* **2013**, *442*, 187.
15. Ballengee, J. B.; Pintauro, P. N. *Macromolecules* **2011**, *44*, 7307.
16. Choi, J.; Lee, K. M.; Wycisk, R.; Pintauro, P. N.; Mather, P. T. *J. Mater. Chem.* **2010**, *20*, 6282.
17. Laforgue, A.; Robitaille, L.; Mokrini, A.; Ajji, A. *Macromol. Mater. Eng.* **2007**, *292*, 1229.
18. Dong, B.; Gwee, L.; Cruz, D. L.; Winey, K. I.; Elabd, Y. A. *Nano Lett.* **2010**, *10*, 3785.
19. Subianto, S.; Pica, M.; Casciola, M.; Cojocaru, P.; Merlo.; Hards, G.; Jones, D. J. *J. Power Sources* **2013**, *233*, 216.
20. Chen, H.; Snyder, J. D.; Elabd, Y. A. *Macromolecules* **2008**, *41*, 128.
21. Mirtalebi, E.; Shirazi, M. M. A.; Kargari, A.; Tabatabaei, M.; Ramakrishna, S. *Desal. Water Treat.* **2014**, *52*, 6611.
22. Shirazi, M. M. A.; Kargari, A.; Bazgir, S.; Tabatabaei, M.; Shirazi, M. J. A. *Desalination* **2013**, *329*, 1.
23. Shirazi, M. J. A.; Bazgir, S.; Shirazi, M. M. A.; Ramakrishna, S. *Desal. Water Treat.* **2013**, *51*, 5974.
24. Cui, W. G.; Li, X. H.; Zhou, S. B.; Weng, J. *J. Appl. Polym. Sci.* **2007**, *103*, 3105.
25. Li, X. Y.; Liu, H. C.; Liu, J. L.; Wang, J. N.; Li, C. *J. Polym. Eng. Sci.* **2012**, *52*, 1964.
26. Zhao, F. W.; Liu, Y.; Yuan, H. L.; Yang, W. M. *J. Appl. Polym. Sci.* **2012**, *125*, 2652.
27. Liu, Y.; Deng, R. J.; Hao, M. F.; Yan, H.; Yang, W. M. *Polym. Eng. Sci.* **2010**, *50*, 2074.
28. Heikkilä, P.; Harlin, A. *Eur. Polym. J.* **2008**, *44*, 3067.